

Transformation from an ultrashort pulse to a spatiotemporal speckle by a thin scattering surface

E. Tal and Y. Silberberg

Department of Physics of Complex Systems, Weizmann Institute of Science, Rehovot 76100, Israel

Received July 24, 2006; revised September 11, 2006; accepted September 11, 2006;
posted September 18, 2006 (Doc. ID 73342); published November 9, 2006

We have theoretically and experimentally studied the local temporal and spectral characteristics of an ultrashort pulse passing a simple thin diffusive element. We show that as one moves away from the diffuser the pulse evolves into a spatiotemporal speckle. © 2006 Optical Society of America
OCIS codes: 030.6140, 320.2250.

The field of ultrashort optical pulse generation has seen significant development in the past few years. Pulses as short as 3.4 fs have been generated,¹ and oscillators providing 10 fs pulses are now commercially available. When using optical elements with these broadband pulses, new effects must be considered: besides nonlinear phenomena such as Kerr lensing, self-phase modulation, and nonlinear photo-damage, linear phenomena such as material dispersion and its byproduct, chromatic aberration, which are nonexistent when using CW lasers, have to be taken into consideration. Furthermore, since every diffractive element is inherently wavelength dependent, it induces spatiotemporal coupling.² Temporal distortion of ultrashort pulses is also studied in the framework of imaging through thick highly scattering media,^{3,4} exploiting a temporal window to collect only the early-arriving unscattered light. Mazurenko⁵ theoretically studied the statistical structure of the spectrum of spatially coherent broadband light backscattered by a rough surface. Tomita and Matsumoto⁶ theoretically and experimentally studied two-dimensional speckle in the space and the time domains when a 50 ps pulse propagated through a disordered solid in the multiple-scattering regime.

Recently, our group⁷ proposed and demonstrated a technique for creating a time lens, where a pulse contracts quickly on its way to a *temporal focus* plane and becomes longer as it moves away from it. This arrangement was shown to be useful in particular for nonlinear microscopy. In that work, temporal focusing was achieved with an arrangement similar to a grating compressor.⁸ We have also pointed out that temporal focusing can also be achieved with thin randomly scattering elements. As will be discussed, a pulse scattered from a random diffuser broadens temporally while forming the temporal equivalent of a spatial speckle pattern. In this Letter we experimentally investigate the effects of a thin random scattering surface on both the temporal and spectral properties of an ultrashort pulse. We also give a simplified geometrical optics calculation of the ensemble-averaged temporal evolution of the pulse, unlike in other works,⁵ where more elaborate statistical parameters of the spectrum were calculated at a location far from the scattering surface. The analogy be-

tween temporal speckles and the more known spatial speckles is also discussed.

Figure 1(b) depicts a geometrical optics picture of the various rays emerging from a thin diffusive surface. When a short pulse of duration τ illuminates the diffuser, each point scatters the light in many directions. For temporal focusing, a telescope forms an image of the diffuser where the image plane is also the location of the temporal focus. Each point in the image plane is also illuminated for duration τ , since all light rays emerging from a single point in the object travel identical optical path lengths and reach the image at the same time, a concept known as Fermat's principle. However, any other point P at some distance from the diffuser, and therefore its image point P', are illuminated for a longer duration dictated by the different trajectories taken by the rays reaching it [see Fig. 1(b)]. The farther P is from the scatterer (or P' from the image plane of the diffuser), the longer the illumination time. Hence, points in front or in the back of the image plane see extended illumination. If we assume an infinitely short pulse impinging on the diffuser, from Fig. 1(b) it is evident that the duration of illumination of point P is given by $\tau(z) = |z|/c(1/\cos\phi - 1)$, where z is the axial distance from P to the diffuser plane, ϕ is half the maxi-

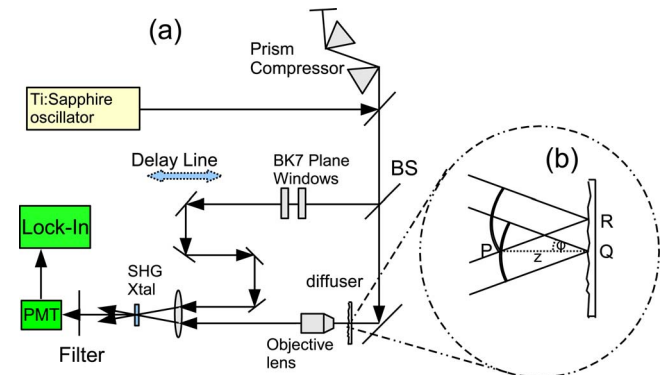


Fig. 1. (Color online) (a) Experimental setup: the field at different locations on the optical axis near the diffuser is imaged onto the SHG crystal via an objective lens and a 100 mm lens. A probe beam with controllable delay samples the image of point P both spatially and temporally. BS, beam splitter; PMT, photomultiplier tube. (b) Geometrical optics description of pulse lengthening: light emanating from Q arrives at P before light emanating from R. Therefore point P experiences extended illumination.

mal scattering angle of the diffuser, and c is the speed of light in the imaging medium. The pulse duration increases with increasing z until $z=D/\tan\phi$, where D is the spot size on the diffuser. Then, the path-length difference between the on-axis and the marginal rays is the biggest. This geometrical optics picture can be used to approximate the pulse characteristics at some distance z for an incoming pulse $I_{\text{inc}}(t)$ before the diffuser. To estimate the average impulse response, we assume that waves emanating from different scatterers are incoherent and have a spherical wavefront inside the cone defined by ϕ . Summing (incoherently) the contributions from all scatterers, we get

$$\langle I(z,t) \rangle = \int_0^{z \tan \phi} \frac{I\left(t - \frac{\sqrt{z^2 + \rho^2}}{c}\right)}{z^2 + \rho^2} 2\pi\rho d\rho, \quad (1)$$

where ρ is the axial distance between the scatterer and the optical axis. Taking $I_{\text{inc}} = \delta(t)$, the impulse response function at a distance z is

$$\langle h(t) \rangle \propto \begin{cases} \frac{1}{t} & \frac{z}{c} \leq t \leq \frac{z}{c \cos \phi} \\ 0 & \text{otherwise} \end{cases}. \quad (2)$$

We note that the calculations only provide an ensemble average of the impulse response, while the exact temporal pattern at each point will depend on the random phases of all components, leading to a specklelike temporal function riding on this incoherent average. In the case of a relatively small range of scattering angles, this approximation is not valid, since the field can no longer be considered uniform across the scattering cone. Instead, a paraxial Gaussian approximation can be adopted. In this approximation we assume a distribution of randomly phased Gaussian beam sources of a finite radius $w_0 = \lambda_0 / \pi\phi$, where λ_0 is the center wavelength. When imaging planes at a distance much greater than the confocal parameter $2z_r = 2\pi w_0^2 / \lambda_0$ from the scattering surface, the effects of the Guoy phase can be neglected, and following the same line of reasoning that led us to Eq. (1) we have

$$\langle I_{\text{parax}}(z,t) \rangle = \int_0^\infty I\left[t - \frac{z}{c} \left(1 + \frac{\rho^2}{2z^2}\right)\right] \exp\left[\frac{-2\rho^2}{w(z)^2}\right] \times \frac{2\pi w_0^2 \rho d\rho}{w(z)^2}, \quad (3)$$

where $w(z) = w_0 \sqrt{1 + (z/z_r)^2}$. This leads to the paraxial impulse response

$$\langle h_{\text{parax}}(t) \rangle \propto \begin{cases} \frac{zc}{w(z)^2} \exp\left[-\frac{4z^2\left(\frac{tc}{z} - 1\right)}{w(z)^2}\right] & t > \frac{z}{c} \\ 0 & \text{otherwise} \end{cases}. \quad (4)$$

To verify this model we performed both numerical wave propagation simulations and an experiment. The experimental setup is shown in Fig. 1(a). As the ultrafast pulse source we used a home-built Ti:sapphire oscillator providing 30 fs pulses centered around 820 nm. The light is collimated to a 2.5 mm spot at the diffuser plane. We used a $2\phi = 10^\circ$ thin holographic diffuser (Newport Corporation) as the random phase plate. The field near the diffuser is imaged using a $10\times$ NA=0.25 objective lens and a 100 mm lens onto a second-harmonic generation (SHG) crystal. We chose the objective lens so that $\text{NA} > \sin\phi$; therefore all the light emanating from P reaches the image plane. A second probe beam with controllable delay is focused using the same 100 mm lens onto the crystal to create a $30\ \mu\text{m}$ spot on the SHG crystal. The probe beam serves both as a temporal and a spatial probe: due to the sixfold magnification of the imaging system the probe beam samples a spot of about $5\ \mu\text{m}$ of the signal beam. Two 6 mm BK7 windows were added to the probe path to balance the dispersion of the two paths. A prism compressor⁹ is used to compensate for the overall dispersion of the system. The SHG signal is measured by a photomultiplier tube. The current generated by the photomultiplier is amplified by use of a lock-in amplifier. For spectral measurements, the SHG crystal is replaced by a single-mode fiber connected to a spectrum analyzer.

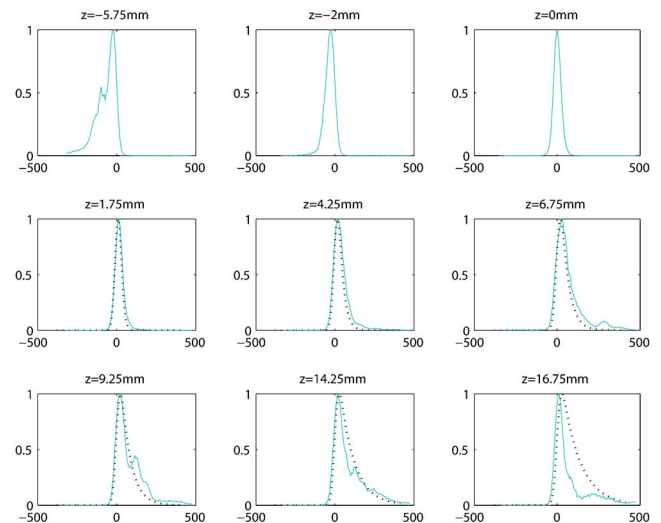


Fig. 2. (Color online) Cross-correlation data taken at different locations on the optical axis. The horizontal axis is given in femtoseconds. z is the distance between the focus of the objective lens and the diffuser. Positive z values indicate a larger distance between the objective lens and the diffuser. For the six bottom traces (positive z values), the dotted curves show the theoretical ensemble average calculated using the paraxial geometrical optics model (see text).

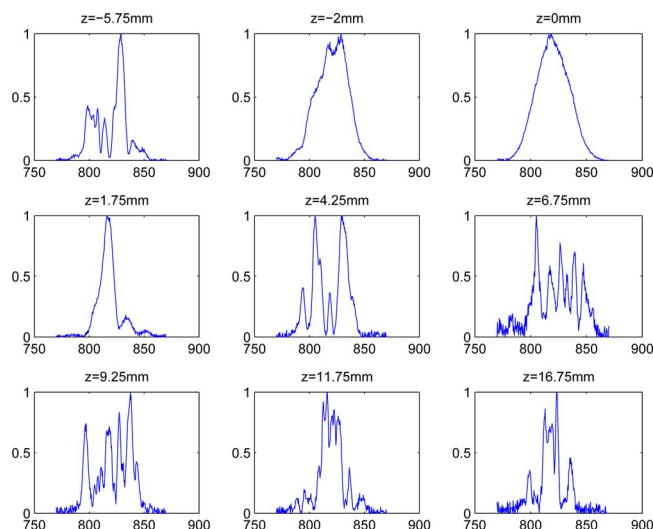


Fig. 3. (Color online) Spectral data taken at different locations on the optical axis. The correlation between adjacent spectral components decreases as we image points further from the diffuser plane. The horizontal axis is the wavelength in nanometers.

Cross-correlation traces and the power spectrum were measured in several locations on the optical axis at intervals of $125\ \mu\text{m}$. Figure 2 shows cross-correlation traces for various locations on the optical axis, scaled to their maximum values. When the plane of the diffuser is imaged (Fig. 2, $z=0\ \text{mm}$) the pulse is at its shortest duration. However, when we move the objective toward the diffuser, the image plane lies behind the SHG crystal. In that case, light arriving from scatterers away from the optical axis on the diffuser reaches the point P' (on the SHG crystal) before light arriving from scatterers on the diffuser near the optical axis. Indeed, as is evident from Fig. 2, at $z=-5.75\ \text{mm}$, $z=-2\ \text{mm}$, the cross-correlation traces grow a tail toward earlier times. When the objective moves away from the diffuser, light arriving from scatterers on the diffuser near the optical axis reaches the SHG crystal first and the tail grows toward later times (Fig. 2, $z=1.75\ \text{mm}$, $z=4.25\ \text{mm}$, and $z=6.75\ \text{mm}$). For the six cross-correlation traces at positive z values of Fig. 2, calculated cross-correlation traces based on the paraxial geometrical optics model are shown by dotted curves. Remember that this model gives the averaged temporal response. We have also performed a more rigorous wave optics numerical simulation taking a randomly generated diffuser that has the same characteristics as the one used in the experiment. The results (not shown) indeed produce temporal speckles similar in features to those observed in the experiment.

The speckling effect is more evident in the power spectrum measurements: when imaging the diffuser plane on the fiber, the power spectrum is identical to

the original laser spectrum (Fig. 3, $z=0\ \text{mm}$). When imaging planes farther away, the spectrum becomes noisy—the correlation between adjacent spectral components decreases. The spectral domain behavior of the pulse is analogous to the well-known space domain dependence of the speckle size when one is observing the speckle field near a diffuser, and the line of reasoning that explains both phenomena is the same: when the plane of the diffuser is imaged, there are no intensity variations in the image because the diffuser is merely a phase element and every image point images an individual scatterer. However, as we move away from the diffuser, domains of bright and dark regions begin to form. The farther we are from the diffuser, the smaller a typical domain size becomes. The typical domain size (correlation length) decreases because more and more random scatterers contribute to a single point in the plane that is imaged. An analogy can also be seen between the time domain and the K-space picture for ordinary speckles: at the diffuser plane the intensity is uniform and only the zero (DC) frequency is present. As we move further away, larger spatial frequencies will begin to appear as tails of the zero spatial frequency component, similar to the cross-correlation traces in the time domain.

In summary, we have shown that a thin diffuser distorts the temporal and spectral behavior of an ultrashort pulse as well as its spatial properties, due to the different optical path lengths of various rays scattered by the diffuser. We have modeled the effects of the diffuser based on a geometrical optics approach and explained the similarities and the source of discrepancy between this simplified model and experiment.

We gratefully acknowledge financial support by the Israel Science Foundation. E. Tal's e-mail address is feeran@weizmann.ac.il.

References

1. K. Yamane, Z. Zhang, K. Oke, R. Morita, and M. Yamashita, *Opt. Lett.* **28**, 2258 (2003).
2. S. Akturk, X. Gu, P. Gabole, and R. Trebino, *Opt. Express* **13**, 8642 (2005).
3. N. C. Bruce, F. E. W. Schmidt, J. C. Dainty, N. P. Barry, S. C. W. Hyde, and P. M. W. French, *Appl. Opt.* **34**, 5823 (1995).
4. F. Liu, K. M. Yoo, and R. R. Alfano, *Opt. Lett.* **19**, 740 (1993).
5. Yu. T. Mazurenko, *Opt. Spectrosc. (USSR)* **66**, 227 (1989).
6. M. Tomita and T. Matsumoto, *J. Opt. Soc. Am. B* **12**, 170 (1995).
7. D. Oron, E. Tal, and Y. Silberberg, *Opt. Express* **13**, 1469 (2005).
8. O. E. Martinez, *IEEE J. Quantum Electron.* **23**, 59 (1987).
9. R. L. Fork, O. E. Martinez, and J. P. Gordon, *Opt. Lett.* **9**, 150 (1984).